

## Higgs bosons decay into bottom-strange in two Higgs Doublet Models

Abdesslam Arhrib

Département de Mathématiques, Faculté des Sciences et Techniques  
B.P. 416 Tanger, Morocco.

and

LPHEA, Département de Physique, Faculté des Sciences-Semlalia,  
B.P. 2390 Marrakech, Morocco.

### Abstract

We analyze the decays  $h^0, H^0, A^0 \rightarrow sb$  within two Higgs Doublet Models with Natural Flavor Conservation (2HDM) type I and II. It is found that the Higgs bosons decay into bottom-strange can lead to a branching ratio in the range  $10^{-4} - 7 \cdot 10^{-4}$  for small  $\tan\beta$  and rather light charged Higgs for both 2HDM-I and 2HDM-II. When  $\tan\beta > 1$ , one can easily reach a branching ratio of the order  $10^{-5}$ . In 2HDM-II, if we impose  $b \rightarrow s$  constraint, we obtain  $Br(h^0 \rightarrow sb)$  of the order  $10^{-5} - 10^{-6}$ . A comparison between the rates of  $h^0 \rightarrow sb$  and  $h^0 \rightarrow cs$  is made. It is found that in the fermophobic scenario,  $h^0 \rightarrow cs$  is still the dominant decay mode.

# 1 Introduction

One of the goals of the next generation of high energy colliders, such as the large hadron collider LHC [1] or the linear collider LC [2] or muon colliders, is to probe top flavor-changing neutral couplings 'top FCNC' as well as the Higgs flavor-changing neutral couplings Higgs FCNC'. FCNC of heavy quarks have been intensively studied both from the theoretical and experimental point of view. Such processes are being well established in the Standard Model (SM) and are excellent probes for the presence of new physics effects such as Supersymmetry, extended Higgs sector and extra fermion families.

Within the SM, with one Higgs doublet, the FCNC  $Ztc$  vanishes at tree-level by the GIM mechanism, while the  $tc$  and  $gtc$  couplings are zero as a consequence of the unbroken  $SU(3)_c \times U(1)_{em}$  gauge symmetry. The Higgs FCNC  $Htc$  and  $Hsb$  couplings also vanish due to the existence of only one Higgs doublet. Both top FCNC and Higgs FCNC are generated at one loop level by charged current exchange, but they are very suppressed by the GIM mechanism. The calculation of the branching ratios for top decays yields the SM predictions [3], [4]:

$$\begin{aligned} Br(t \rightarrow Zc) &= 1.3 \cdot 10^{-13}; Br(t \rightarrow c\gamma) = 4.3 \cdot 10^{-13}; Br(t \rightarrow gc) = 3.8 \cdot 10^{-11}; \\ Br(t \rightarrow Hc) &= 5.6 \cdot 10^{-14} \quad \text{for} \quad M_H = 115 - 130 \text{ GeV} : \end{aligned} \quad (1)$$

While for Higgs FCNC, calculation within SM leads to:

$$\begin{aligned} Br(H \rightarrow sb) &= 10^{-7} \text{ (resp } 10^{-9}) \text{ } m_H = 100 \text{ (resp } 200) \text{ GeV} \\ Br(H \rightarrow tc) &= 1.5 \cdot 10^{-16} \text{ (resp } 3 \cdot 10^{-13}) \text{ } m_H = 200 \text{ (resp } 500) \text{ GeV} \end{aligned} \quad (2)$$

Many SM extensions predict that these top and Higgs FCNC can be orders of magnitude larger than their SM values. For the Higgs FCNC, an important class of models where Higgs FCNC appear at tree level are the so called two Higgs doublet models without Natural Flavor Conservation (NFC) 2HDM-III [5, 6, 7, 8]. In this class of models, the branching ratio of  $h \rightarrow tc$  can be larger than 10% in some cases [6]. In the framework of 2HDM with NFC type I and II, top and Higgs FCNC have been studied in [9]. It was shown that in 2HDM-II the  $Br(h \rightarrow tc)$ ,  $h = h^0$  or  $H^0$ , may reach  $10^{-5}$  for CP-even states. This rate is almost eight orders of magnitude larger than the SM one.

Recently, Higgs FCNC couplings have been addressed also in supersymmetry [10, 11, 12]. In those studies it has been shown that  $Br(h^0 \rightarrow sb)$  can be in the range of  $10^{-4}$ - $10^{-3}$ . This rate originates mainly from the flavor violation interactions mediated by the gluino [10, 12].

Hence, Higgs FCNC offer a good place to search for new physics, which may manifest itself if those couplings are observed in future experiments such as LHC or LC [1, 2]. Therefore, models which can enhance those FCNC couplings are welcome.

The aim of this paper is to study Higgs FCNC couplings such as  $h \rightarrow sb$ ,  $h = h^0; H^0; A^0$ , in the framework of NFC two Higgs doublet models type I and II. It is found that the branching ratios of  $Br(h \rightarrow sb)$ ,  $h = h^0; H^0; A^0$ , can be greater than  $> 10^{-5}$  in quite a substantial region of the 2HDM parameter space.  $Br(h \rightarrow tc)$  requires large  $\tan\beta$  and

light charged Higgs [9] while  $\text{Br}(\tau \rightarrow \text{sb})$  requires rather small  $\tan\beta$  together with light charged Higgs and large soft breaking term  $m_{5}$ .

The paper is organized as follows. In the next section, the 2HDM is introduced. Relevant couplings are given, and theoretical and experimental constraints on 2HDM parameters are discussed. In the third section, we will study the effects of 2HDM on  $\text{Br}(\tau \rightarrow \text{sb})$  which are evaluated in 2HDM-I and 2HDM-II. Our conclusion is given in section 4.

## 2 The 2HDM

Two Higgs Doublet Models (2HDM) are formed by adding an extra complex  $SU(2)_L \times U(1)_Y$  scalar doublet to the SM Lagrangian. Motivations for such a structure include CP violation in the Higgs sector and the fact that some models of dynamical electroweak symmetry breaking yield the 2HDM as their low-energy effective theory [13].

The most general 2HDM scalar potential which is both  $SU(2)_L \times U(1)_Y$  and CP invariant is given by [14]:

$$V(\phi_1, \phi_2) = \frac{1}{2}(\mu_1^2 - \lambda_1^2 v_1^2) \phi_1^\dagger \phi_1 + \frac{1}{2}(\mu_2^2 - \lambda_2^2 v_2^2) \phi_2^\dagger \phi_2 + \frac{1}{2}(\lambda_3^2 (\phi_1^\dagger \phi_2 + \phi_2^\dagger \phi_1) + \lambda_4^2 (\phi_1^\dagger \phi_2 - \phi_2^\dagger \phi_1)^2) + \frac{1}{2}(\lambda_5^2 (\phi_1^\dagger \phi_2 - \phi_2^\dagger \phi_1)^2) + \frac{1}{2}(\lambda_6^2 (\phi_1^\dagger \phi_2 + \phi_2^\dagger \phi_1)^2) + \frac{1}{2}(\lambda_7^2 (\phi_1^\dagger \phi_2 - \phi_2^\dagger \phi_1)^2) + \frac{1}{2}(\lambda_8^2 (\phi_1^\dagger \phi_2 + \phi_2^\dagger \phi_1)^2) \quad (3)$$

where  $\mu_1$  and  $\mu_2$  have weak hypercharge  $Y=1$ ,  $v_1$  and  $v_2$  are respectively the vacuum expectation values of  $\phi_1$  and  $\phi_2$  and the  $\lambda_i$  are real valued parameters. Note that this potential violates the discrete symmetry  $\phi_1 \rightarrow -\phi_1$  softly by the dimension two term  $\lambda_5 < (\phi_1^\dagger \phi_2)$ . The above scalar potential has 8 independent parameters ( $\lambda_i$ ) $_{i=1,\dots,6}$ ,  $v_1$  and  $v_2$ . After electroweak symmetry breaking, the combination  $v_1^2 + v_2^2$  is thus fixed by the electroweak scale through  $v_1^2 + v_2^2 = (2^{\sqrt{2}} G_F)^{-1}$ . We are left then with 7 independent parameters.

Meanwhile, three of the eight degrees of freedom of the two Higgs doublets correspond to the 3 Goldstone bosons ( $G^\pm, G^0$ ) and the remaining five become physical Higgs bosons:  $H^\pm$ ,  $h^0$  (CP even),  $A^0$  (CP odd) and  $H^0$ . Their masses are obtained as usual by diagonalizing the mass matrix. The presence of charged Higgs bosons will give new contributions to the one-loop induced FCNC couplings, as shown in Fig. (1)  $d_{11} \dots d_{18}$ .

It is possible to write the  $\lambda_i$  in terms of physical scalar masses,  $\tan\beta$ , and  $\lambda_5$  (see [15] for details). We are then free to take as 7 independent parameters ( $\lambda_i$ ) $_{i=1,\dots,6}$  and  $\tan\beta$  or equivalently the four scalar masses,  $\tan\beta$ , and one of the  $\lambda_i$ . In what follows we will take  $\lambda_5$  as a free parameter as well as the physical masses and mixing.

We list hereafter the Feynman rules in the general 2HDM for the trilinear scalar couplings relevant for our study. They are written in terms of the physical masses,  $\tan\beta$ , and the soft breaking term  $m_{5}$ :

$$H^0 H^\pm H^\pm = \frac{ig}{M_W \sin 2\beta} (M_{H^0}^2 (\cos^3 \beta \sin \beta + \sin^3 \beta \cos \beta) + M_H^2 \sin 2\beta \cos(\alpha - \beta)) \sin(\alpha + \beta) \frac{m_5^2}{v^2} \quad (4)$$

$$H^0 H^+ G = \frac{ig}{2M_W} \sin(\alpha) (M_{H^0}^2 - M_H^2) \quad (5)$$

$$h^0 H^+ H = \frac{ig}{M_W \sin 2\beta} (M_{h^0}^2 (\cos^2 \alpha \cos^2 \beta - \sin^2 \alpha \sin^2 \beta) + M_H^2 \sin 2\alpha \sin(\alpha - \beta)) \cos(\alpha + \beta) \sqrt{s} v^2 \quad (6)$$

$$h^0 H^+ G = \frac{ig}{2M_W} \cos(\alpha) (M_{h^0}^2 - M_H^2) \quad (7)$$

$$A^0 H^+ G = \frac{g}{2M_W} (M_H^2 - M_A^2) \quad ; \quad v^2 = \frac{2M_W^2}{g^2} \quad (8)$$

We need also the couplings of scalar boson to a pair of fermions both in 2HDM -I and 2HDM -II. In those couplings, the relevant terms are as follows:

$$h^0 tt / M_t \frac{\cos \alpha}{\sin \beta} \quad ; \quad H^0 tt / M_t \frac{\sin \alpha}{\sin \beta} \quad ; \quad A^0 tt / \frac{M_t}{\tan \beta} \quad \text{2HDM -I; II} \quad (9)$$

$$(H^\pm bt)_L / \frac{M_b}{\tan \beta} \quad ; \quad (H^\pm bt)_R / \frac{M_t}{\tan \beta} \quad \text{2HDM -I} \quad (10)$$

$$(H^\pm bt)_L / M_b \tan \beta \quad ; \quad (H^\pm bt)_R / \frac{M_t}{\tan \beta} \quad \text{2HDM -II} \quad (11)$$

In this analysis, we take into account the following constraints when the independent parameters are varied. From the theoretical point of view:

i) The contributions to the  $\rho$  parameter from the Higgs scalars [16] should not exceed the current limits from precision measurements [17]:  $|\rho - 1| < 0.001$ . We stress in passing that in order to satisfy the  $\rho$  constraint we take  $M_H = M_A$  which gives  $\alpha = \beta$ . It is easy to show that when  $M_H = M_A$  the extra contribution to  $\rho$  vanish. Under this constraint the 2HDM scalar potential is O(4) symmetric [18]. In this case  $(H^+, A^0; H^0)$  form a triplet under the residual global SU(2) of the Higgs potential. It is this residual symmetry which ensures that  $\rho$  is equal to unity at tree level.

ii) From the requirement of perturbativity for the top and bottom Yukawa couplings [19],  $\tan \beta$  is constrained to lie in the range  $0.1 < \tan \beta < 70$ .

iii) It has been shown in [20] that for models of the type 2HDM -II, data on  $b \rightarrow s$  imposes a lower limit of  $M_H > 280 \text{ GeV}$ . In type I 2HDM, there is no such a constraint on charged Higgs mass [20]. In our numerical analysis we will ignore this constraint in order to localize regions in the 2HDM parameter space where the branching ratios are sizeable.

iv) Unitarity and perturbativity constraints on scalar parameters:

It is well known that the unitarity bounds coming from a tree-level analysis [21, 22] put severe constraints on all scalar trilinear and quartic couplings. The tree level unitarity bounds are derived with the help of the equivalence theorem, which itself is a high-energy approximation where it is assumed that the energy scale is much larger than the  $Z^0$  and  $W$  gauge-boson masses. We will use, instead of unitarity constraints, the perturbativity constraints by assuming that all  $\lambda_i$  satisfy:

$$|\lambda_{ij}| \leq 4 \quad (12)$$

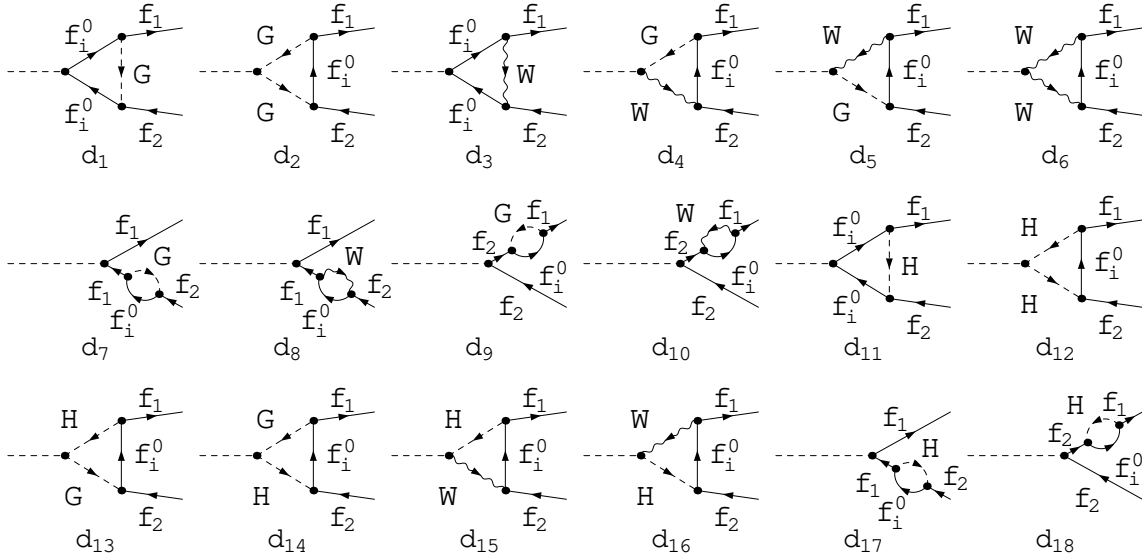


Figure 1: Generic contribution to  $f_1 f_2$  in SM  $d_1 - d_{10}$ , in 2HDM  $d_{11} - d_{18}$

Those perturbative constraints on the  $\Gamma_i$  allow us to investigate a larger parameter space than the one allowed by unitarity constraints.

We would like to mention also that when performing the scan over the 2HDM parameter space, we realize that for some points the widths of the scalar particles become bigger than their corresponding masses:  $\Gamma_i > M_i$  ( $i = h^0; H^0; A^0; H^\pm$ ). This happens both when we impose tree level unitarity constraints and/or perturbativity constraints. The width becomes large specially when the pure scalar decays like  $H^0 \rightarrow h^0 h^0, H^0 \rightarrow H^+ H^-, h^0 \rightarrow H^+ H^-, H^0 \rightarrow A^0 A^0$  and  $h^0 \rightarrow A^0 A^0$  are open. We find it is natural to add to the above constraints the requirement that the width of the scalar particles remains smaller than the mass of the corresponding particles:

$$\Gamma_i < M_i \quad (13)$$

From the experimental point of view, the combined null searches from all four CERN LEP collaborations derive the lower limit  $M_H > 78.6 \text{ GeV}$  (95% CL), a limit which applies to all models in which  $\text{BR}(H \rightarrow \text{hadrons}) + \text{BR}(H \rightarrow \text{leptons}) = 1$ . For the neutral Higgs bosons, OPAL collaboration has put a limit on  $h^0$  and  $A^0$  masses of the 2HDM. They conclude that the regions  $1 < M_h < 44 \text{ GeV}$  and  $12 < M_A < 56 \text{ GeV}$  are excluded at 95% CL independent of  $\tan\beta$  and  $\mu$  [23]. For simplicity we will assume that all scalar particles masses are  $> 100 \text{ GeV}$ .

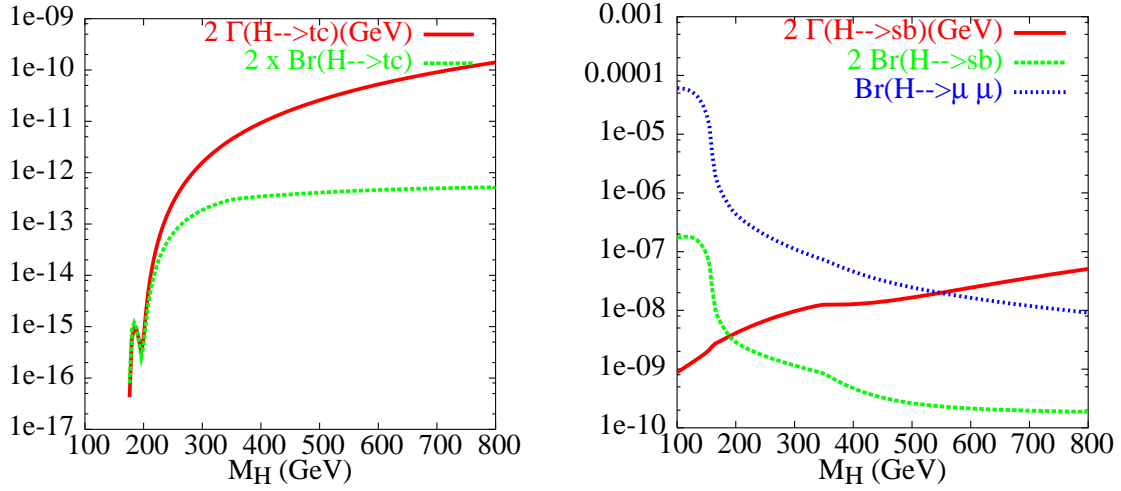


Figure 2: SM width and Branching ratio for  $H \rightarrow tc$  (left) and  $H \rightarrow sb$  (right) as a function of Higgs mass.

### 3 Higgs FCNC in 2HDM

#### 3.1 Higgs FCNC in SM

Before presenting our results in 2HDM, we would like to give the branching ratio of  $H \rightarrow tc$  and  $H \rightarrow sb$  in the SM. To our best knowledge, the first calculation for  $\text{Br}(H \rightarrow sb)$  has been carried out in [24]. However, in [24], numerical results have been given only for a very light Higgs boson  $M_H = 9 \text{ GeV}$ . Recently a new estimation, using dimensional analysis and power counting, has appeared both for  $\text{Br}(H \rightarrow sb)$  [12] and  $\text{Br}(H \rightarrow tc)$  [9]. Here we present exact result based on diagrammatic calculations both for  $\text{Br}(H \rightarrow sb)$  and  $\text{Br}(H \rightarrow tc)$ . We give numerical results for the width as well as for the branching ratio. The Feynman diagrams contributing to those process in SM are depicted in Fig. (1)  $d_1$  to  $d_{10}$ . In the case of  $H \rightarrow tc$ , in Fig. (1)  $(f_1; f_2) = (t; c)$  and  $f_i^0 = d; s; b$ , while for  $H \rightarrow sb$   $(f_1; f_2)$  is  $(b; s)$  and  $f_i^0 = u; c; t$ . The full loop calculation presented here is done with the help of FormCalc [25]. FF and LoopTools packages [26] are used in numerical analysis. The numerical results shown in eqs. (1,2) is derived by FormCalc [25].

In the SM, as expected, the branching ratio of  $H \rightarrow tc$  and  $H \rightarrow sb$  are very suppressed due to GIM mechanism. The branching ratio is very small in both cases for higher Higgs mass  $M_H \gg 2M_Z$  where  $H \rightarrow W^+W^-$  and  $H \rightarrow Z^0Z^0$  are open.

Both in SM and 2HDM, the decay widths  $\Gamma^{\text{SM}}$  and  $\Gamma^{2\text{HDM}}$  of scalar particles:  $H = H^{\text{SM}}$ ,  $h^0, H^0, A^0$  and  $H^\pm$  are computed at tree level as follows:

$$\Gamma^{\text{SM}} = \sum_f \left( \Gamma(f f) + \Gamma(VV) \right)$$

$$\Gamma^{2\text{HDM}} = \sum_f \left( \Gamma(f f) + \Gamma(VV) + \Gamma(VH_i) + \Gamma(H_i H_j) \right) \quad (14)$$

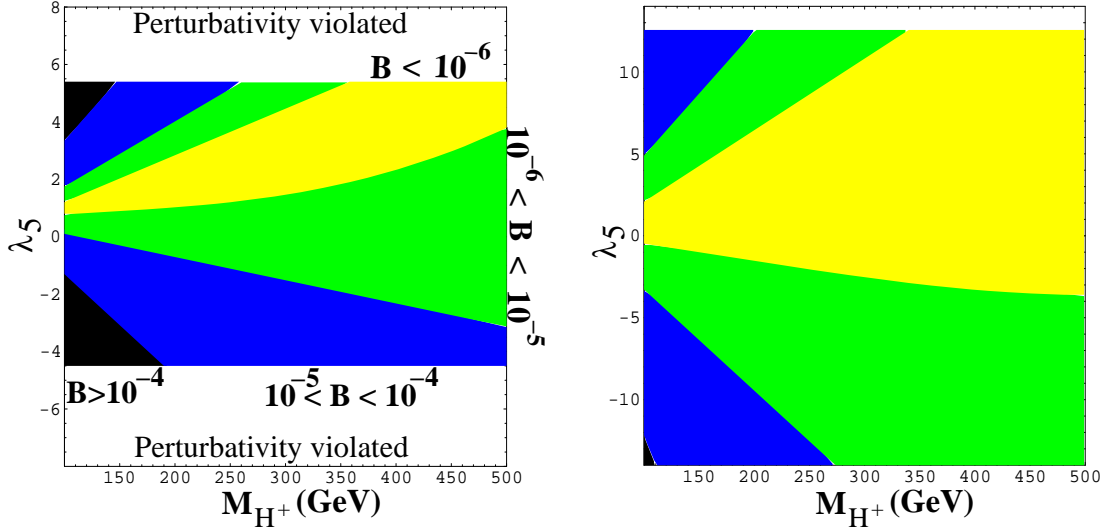


Figure 3: Contours for  $2 \text{ Br}(h^0 \rightarrow sb)$  in 2HDM -II  $\tan \beta = 0.3$  (left),  $\tan \beta = 1.5$  GeV (right) in the  $(M_{H^+}, \lambda_5)$  plane with  $M_h = 110, M_H = 180$  GeV,  $\sin \beta = 0.1$  and  $M_{A^0} = M_H$

QCD corrections to  $\Gamma \rightarrow f\bar{f}$  and  $\Gamma \rightarrow f\bar{g}g$ ;  $\Gamma \rightarrow Z; V \rightarrow V; VV; V H_i g$  decays are not included in the widths. The decay widths of the Higgs bosons are taken from [27].

For a Higgs mass heavier than 250 GeV, we get branching ratio of the order  $10^{-14}$  to  $10^{-12}$  (resp  $10^{-10}$  to  $10^{-9}$ ) for  $H \rightarrow t\bar{c}$  (resp  $H \rightarrow sb$ ). In the case of  $H \rightarrow sb$ , the branching ratio is enhanced for Higgs boson mass of the order  $M_H = 100$  to  $120$  GeV where the width of the Higgs is very narrow. We have plotted in Fig. (2) both the decay width and the branching ratios of  $H \rightarrow t\bar{c}$  (left plot) and  $H \rightarrow sb$  (right plot) as well as the branching ratio of  $H \rightarrow \tau^+\tau^-$ . As it can be seen from the right plot  $\text{Br}(H \rightarrow sb)$  is two orders of magnitude smaller than  $\text{Br}(H \rightarrow \tau^+\tau^-)$ .

### 3.2 $h^0 \rightarrow sb$

Turning now to the 2HDM Higgs bosons FCNC couplings  $\Gamma \rightarrow sb, \Gamma = h^0; H^0; A^0$ . The Feynman diagrams are depicted in Fig. (1). The amplitude is sensitive to the  $H^+H^-$  and  $H^\pm G$  couplings through diagrams  $d_{12,13,14}$  as well as to the  $t\bar{t}$  and  $(H^\pm b\bar{t})_{L,R}$  couplings through diagrams  $d_{11,12,13,14}$ . It is clear from equation (9) that the top effect is enhanced for small  $\tan \beta$  in the case of CP-odd  $A^0$  boson. While in the case of CP-even  $H^0$  and  $h^0$ , the couplings are enhanced at small  $\tan \beta$  and large  $\sin \beta$  (resp large  $\cos \beta$ ) for  $H^0$  (resp  $h^0$ ). Consequently, our numerics are presented for small  $\tan \beta = 0.3$ ,  $\sin \beta = 0.1$  for  $h^0 \rightarrow sb$  and  $\sin \beta = 0.95$  for  $H^0 \rightarrow sb$ .

We show in Fig. (3) contour plots for  $\text{Br}(h^0 \rightarrow sb)$  in 2HDM -II  $\tan \beta = 0.3$  (left) and  $\tan \beta = 1.5$  GeV (right) in the  $(M_{H^+}, \lambda_5)$  plane.  $\lambda_5$  is varied in the perturbative range  $|\lambda_5| < 4$ . The other inputs are  $M_h = 110, M_H = 180$  GeV,  $\sin \beta = 0.1$  and  $M_{A^0} = M_H$ . The width  $\Gamma_{h^0}$  is computed at tree level according to eq. (14). Since the mass of  $h^0$  is taken

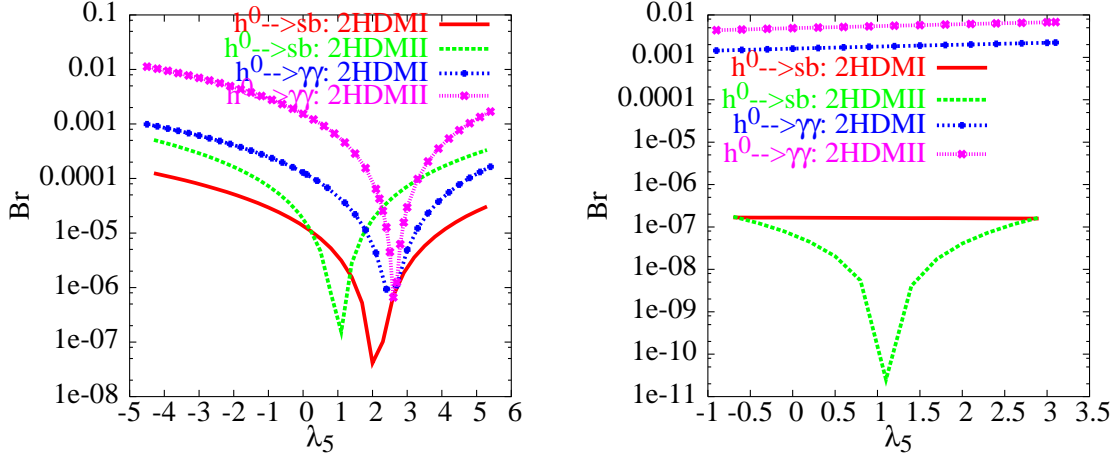


Figure 4:  $Br(h^0 \rightarrow sb)$  and  $2 Br(h^0 \rightarrow \gamma\gamma)$  in 2HDM –I and II,  $m_H = 100$  GeV,  $\tan\beta = 0.3$  (left) and  $\tan\beta = 5$  (right). All the other parameters are the same as in Fig. (3).

at 110 GeV, only light fermions contribute to  $\Gamma_{h^0}$  and so the width is very narrow and is of the order  $57 \cdot 10^4$  (resp  $83 \cdot 10^5$  GeV) at  $\tan\beta = 0.3$  (resp  $\tan\beta = 1.5$ ). Such narrow width could enhance the branching ratio  $Br(h^0 \rightarrow sb)$ .

We would like to mention first that for this set of parameters, the perturbativity of scalar quartic couplings  $\lambda_i$  is violated around  $\lambda_5 > 5.5$ . We get  $|j_{1j}| > 4$  for  $\tan\beta = 0.3$ , while for  $\tan\beta = 1.5$  there is no such bound.

Large branching ratios can be obtained for light charged Higgs mass. This can be seen in the left panel black and blue areas of Fig. (3) which correspond to small  $\tan\beta = 0.3$  and large  $|j_{5j}|$ . In those areas the coupling  $h^0 H^+ H^-$  gets its largest value (see also Fig. (4)). In this case one can obtain branching ratio in the range:  $10^4 < Br(h^0 \rightarrow sb) < 6 \cdot 10^4$  for  $M_H < 200$  GeV,  $\lambda_5 < 1.2$  and  $\lambda_5 > 3$ . For charged Higgs mass greater than 200 GeV, there is also a region where the branching ratio can be in the range  $10^5 \cdot 10^4$ . This can be achieved by taking large and negative  $\lambda_5 < -1$ . In the case of positive  $\lambda_5$  and  $M_H > 250$  GeV, the branching ratio decreases to a value  $< 10^5$ .

When  $\tan\beta = 1.5$ , the coupling  $h^0 tt$  is reduced, and we are left only with a small region where the branching ratio  $Br(h^0 \rightarrow sb)$  is of the order  $10^5 \cdot 10^4$  for  $M_H < 250$  GeV and large  $|j_{5j}| > 5$ . In both plots (left and right), the coupling  $h^0 H^+ H^-$  reaches its minimal value in the region where  $\lambda_5 = 0 \cdot 2$ , which explains why the branching ratio is so small in this region.

### 3.3 Can $h^0 \rightarrow sb$ compete with $h^0 \rightarrow \gamma\gamma$ ?

It is well known that the decay  $h^0 \rightarrow \gamma\gamma$  is loop induced and so is suppressed. In the SM the branching ratio  $Br(H^{SM} \rightarrow \gamma\gamma)$  is about  $10^{-3}$  for Higgs mass in the range  $M_H = 100 \cdot 160$  GeV. Hence, with maximum branching ratio for  $h^0 \rightarrow sb$  of the order

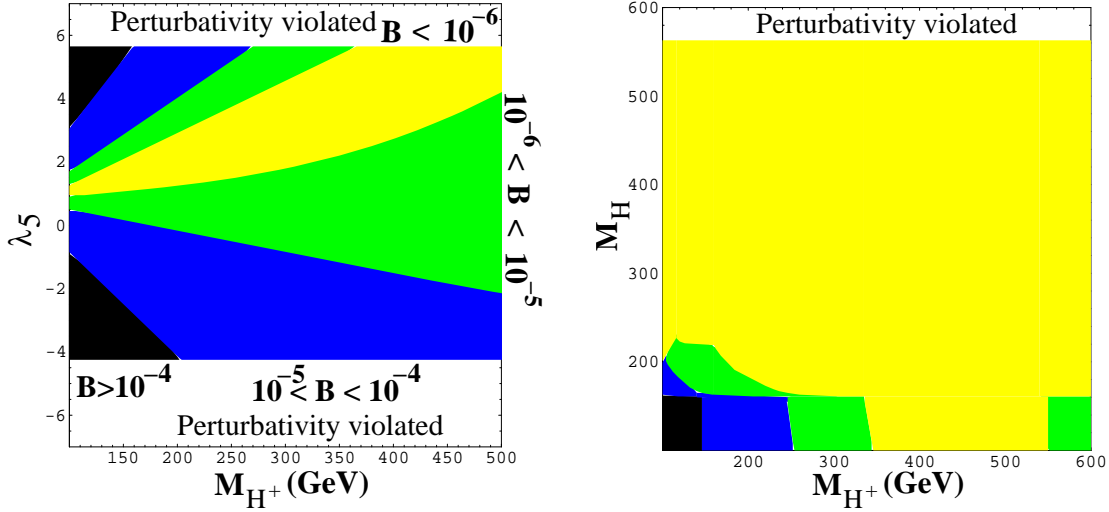


Figure 5: Contours for  $2 \text{ Br}(H^0 \rightarrow sb)$  in 2HDM -II in the plan  $(M_{H^+}, \lambda_5)$   $M_H = 140$  GeV (left),  $(M_{H^+}, M_H)$   $\lambda_5 = 5$  (right) with  $\tan \beta = 0.3$ ,  $M_h = 110$ ,  $\sin \beta = 0.95$  and  $M_{A^0} = M_H$

$10^{-4} \leq 6 \cdot 10^{-4}$  in 2HDM -I or II, it is legitimate to compare  $h^0 \rightarrow sb$  and  $h^0 \rightarrow sb$  in 2HDM -I or II.

We illustrate in Fig. (4) the branching ratio for  $h^0 \rightarrow sb$  and  $h^0 \rightarrow sb$  both in 2HDM -I and II. The charged Higgs mass is fixed to 100 GeV. It is clear that in the case  $\tan \beta = 0.3$   $h^0 \rightarrow sb$  is about one order of magnitude bigger than  $h^0 \rightarrow sb$ . While, in the case of  $\tan \beta = 5$   $h^0 \rightarrow sb$  is more than four orders of magnitude bigger than  $h^0 \rightarrow sb$ . This is because at  $\tan \beta = 0.3$  (resp  $\tan \beta = 5$ ) the  $W$  loop are suppressed by a factor  $h^0 W^+ W^- / \sin(\beta) \approx 0.2$  (resp enhanced by  $h^0 W^+ W^- / \sin(\beta) \approx 0.96$ ). All the dips observed in the plots correspond to the minimum of the coupling  $h^0 H^+ H^-$ . Those dips are not located at the same  $\lambda_5$ , this is due to a destructive interference with others diagrams. An interesting feature of the 2HDM -I, is its fermiophobic limit. The light CP-even Higgs  $h^0$  of the 2HDM -I is fermiophobic in the limit  $\tan \beta = 2$ , all  $h^0$  couplings to fermions vanishes for  $\tan \beta = 2$  [28, 14]. If  $h^0$ , with a mass in the range 100 - 160 GeV, is fermiophobic the dominant decay mode is  $h^0 \rightarrow sb$ . It has been shown in Ref. [29] that in the fermiophobic limit, the branching ratio of the one loop induced decay  $h^0 \rightarrow bb$  is below 10% - 30%. As the decay  $h^0 \rightarrow sb$  is concerned, we have checked by general scan that in the fermiophobic limit, the decay width of  $h^0 \rightarrow sb$  is more than one order of magnitude bigger than the width of  $h^0 \rightarrow sb$ .

In fact, in the 2HDM, not only the coupling  $h^0 \rightarrow sb$  and  $h^0 \rightarrow Z$  [30] can have non decoupling effects, but also one loop contribution to  $h^0 \rightarrow bb$  [31] and  $h^0 \rightarrow h^0 h^0$  [32].

### 3.4 $H^0 \rightarrow sb$

We now discuss the heavy CP-even decay  $H^0 \rightarrow sb$ . Our numerical results are shown in Fig. (5). To maximize the coupling  $H^0 tt$ , we choose of course small  $\tan \beta$  and large  $\sin \beta$ . In the right plot of figure (5), we show contour plots for  $\text{Br}(H^0 \rightarrow sb)$  in the plane  $(M_H; \sin \beta)$  for  $M_H = 140 \text{ GeV}$ . For CP-even Higgs mass  $140 \text{ GeV}$ ,  $H^0 \rightarrow W^+W^-$ ,  $H^0 \rightarrow ZZ$ ,  $H^0 \rightarrow tt$ ,  $H^0 \rightarrow A^0Z$  and  $H^0 \rightarrow H_i H_j$  are not yet open, and so the width is narrow. In particular, for the set of parameters fixed here:  $M_h = 110$ ,  $\sin \beta = 0.95$  and  $M_{A^0} = M_H$ , the width is  $73 \times 10^4 \text{ GeV}$ .

The behavior is similar to what we obtain for  $\text{Br}(h^0 \rightarrow sb)$ . In the black regions (large  $\sin \beta$ ), the coupling  $H^0 H^+ H^-$  is maximal while for  $\sin \beta \in [0; 2]$   $H^0 H^+ H^-$  is minimal. In the black region the branching ratio of  $\text{Br}(H^0 \rightarrow sb)$  can reach  $\sim 7 \times 10^4$ . From the left panel of figure (5), it is evident that there is a relatively large region in the plane  $(M_H; \sin \beta)$  where the  $\text{Br}(H^0 \rightarrow sb) > 10^5$ .

In the right panel of figure (5), we show  $\text{Br}(H^0 \rightarrow sb)$  in the plane  $(M_H; M_{H^\pm})$  for  $\sin \beta = 5$ . One can see that when CP-even mass  $M_H < 2M_W$ , the decay  $H^0 \rightarrow W^+W^-$  is not yet open. The width  $\Gamma_{H^0}$  is narrow, and so the branching ratio is large. For  $M_H < 250 \text{ GeV}$  and  $M_{H^\pm} < 2M_W$ , one can have  $\text{Br}(H^0 \rightarrow sb) > 10^5$ . Once the CP-even Higgs mass  $M_H > 2M_W$ , the decay  $H^0 \rightarrow W^+W^-$  is open, and the width is larger than  $5 \times 10^2 \text{ GeV}$ . The branching ratio  $\text{Br}(H^0 \rightarrow sb)$  is then reduced. As it can be seen from the plot, for  $M_H > 220 \text{ GeV}$ , the branching ratio  $\text{Br}(H^0 \rightarrow sb)$  is less than  $< 10^6$ .

In the case of 2HDM -I, both  $h^0 tt$ ,  $H^0 tt$  and  $(H^+ bt)_R$  couplings are the same as in 2HDM -II, while  $(H^+ bt)_L$  which is proportional to  $M_b \tan \beta$  in 2HDM -II is now proportional to  $M_b = \tan \beta$ . For small  $\tan \beta$ , both  $\text{Br}(h^0 \rightarrow sb)$  and  $\text{Br}(H^0 \rightarrow sb)$  are of the same order as in 2HDM -II, while for large  $\tan \beta$  those branching ratios are less than about  $10^6$ .

### 3.5 $A^0 \rightarrow sb$

Let us now look at 2HDM contribution to  $A^0 \rightarrow sb$ . Since  $A^0$  is CP-odd, it does not couple to a pair of charged Higgs. The only pure trilinear scalar coupling which contributes to  $A^0 \rightarrow sb$  is  $A^0 H^+ G^-$  eq. (8). Unlike the couplings  $H^0 H^+ H^-$  and  $h^0 H^+ H^-$  eqs (4,6), which depend both on Higgs masses,  $\tan \beta$  as well as the soft breaking term  $\mu_5$ , the coupling  $A^0 H^+ G^-$  depends only on the splitting  $M_H^2 - M_A^2$ . As mentioned above, such splitting should not be too large, otherwise the  $\mu_5$  constraint is not satisfied. As one can read from eqs. (9,11), the couplings  $A^0 tt$  and  $(H^+ bt)_R$  are proportional to  $M_t = \tan \beta$ . Hence enhancement is expected at small  $\tan \beta$ .

As we stressed before, our 2HDM parameters in this case are:  $\tan \beta$ ,  $M_A$  and  $M_H$ . For simplification, we use the MSSM sum-rules to fix charged Higgs mass and by using  $\tan \beta$ , CP-odd mass  $M_A$  and a SUSY scale which we take at  $1 \text{ TeV}$ . CP-odd mass will be varied from  $100 \text{ GeV}$  to  $600 \text{ GeV}$  without worrying about perturbativity.  $\tan \beta$  is taken to be  $> 0.1$ .

We present our numerical results for  $A^0 \rightarrow sb$  in 2HDM -II in fig. (6). As can be seen from the left plot, the branching ratio  $\text{Br}(A^0 \rightarrow sb)$  is greater than  $10^5$  only for small

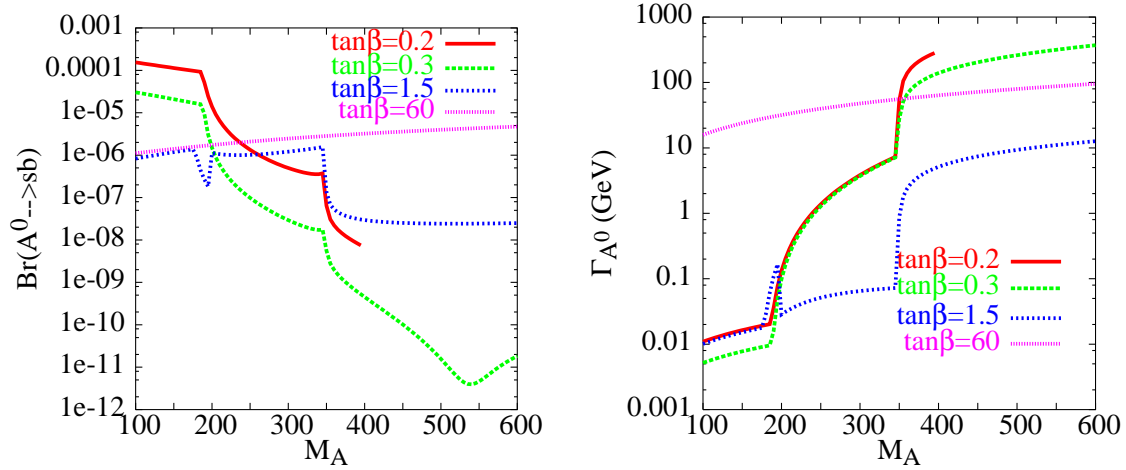


Figure 6: 2  $\text{Br}(A^0 \rightarrow sb)$  (left) and CP-odd  $A^0$  width  $\Gamma_{A^0}$  (right) as function of  $M_A$  for several values of  $\tan\beta$

$\tan\beta = 0.1 \dots 0.35$  and light  $M_A$  and  $M_H$ . For light  $M_A < 200$  GeV and low  $\tan\beta < 1$ , the width of  $A^0$  is still small and so the branching ratio is enhanced. For  $M_A > 200$  GeV, the decay  $A^0 \rightarrow h^0 Z$  is open and the decay width  $\Gamma_{A^0}$  increases. Therefore, the branching ratio is reduced. Note that for  $\tan\beta = 0.2$ , we cut off the curve at  $M_A = 400$  GeV where the width  $\Gamma_{A^0}$  starts to be greater than  $M_A$ . At large  $\tan\beta$ , due to the bottom Yukawa coupling, both the partial width  $\Gamma(A^0 \rightarrow sb)$  and total width  $\Gamma_{A^0}$  are enhanced, and the branching ratio is saturated in the range  $[10^{-6}; 10^{-5}]$ .

The situation is almost the same in 2HDM -I.

## 4 Conclusions

In the framework of the 2HDM with natural flavor conservation, we have studied various Higgs FCNC  $\rightarrow sb$ . The study has been carried out taking into account the experimental constraint on the  $\mu$  parameter and also perturbativity constraints on all the scalar quartic couplings  $\lambda_i$ . Numerical results for the branching ratios have been discussed. We emphasized the effect coming from both top and bottom Yukawa couplings and pure trilinear scalar couplings such as  $h^0 H^+ H^-$  and  $H^0 H^+ H^-$ .

We have shown that, in 2HDM -I and 2HDM -II, the branching ratios of Higgs FCNC  $fh^0; H^0; A^0 g \rightarrow sb$  are enhanced for small  $\tan\beta$ , rather light charged Higgs boson and large soft breaking term  $\mu$ . The branching ratio of  $\text{Br}(fh^0; H^0 g \rightarrow sb)$  can reach the level of  $10^{-4} \dots 7 \cdot 10^{-4}$  which is comparable to size of SUSY predictions [10, 12].

In the case of light CP-even  $m_{h^0} = 100 \dots 160$  GeV, we have also shown that the branching ratio of  $\text{Br}(h^0 \rightarrow sb)$  is well below  $\text{Br}(h^0 \rightarrow \gamma a)$ . This is also the case in the fermiophobic limit of 2HDM -I.

**Acknowledgments** This work was done within the framework of the Associate Scheme of ICTP. Thanks to Thomas Hahn for his help. We also want to thank Andrew Akeroyd for discussions and for reading the manuscript.

## References

- [1] M. Beneke, I. Efthymiopoulos, M. L. Mangano, J. Williams (conveners) et al., report in the Workshop on Standard Model Physics (and more) at the LHC, Geneva, hep-ph/0003033
- [2] J. A. Aguilar-Saavedra et al. [ECFA/DESY LC Physics Working Group Collaboration], arXiv hep-ph/0106315.
- [3] G. Eilam, J. L. Hewett and A. Soni, Phys. Rev. D 44 (1991) 1473 [Erratum -ibid. D 59 (1999) 039901].
- [4] B. Mele, S. Petrarca and A. Soddu, Phys. Lett. B 435, 401 (1998)
- [5] T. P. Cheng and M. Sher, Phys. Rev. D 35, 3484 (1987).
- [6] W. S. Hou, Phys. Lett. B 296, 179 (1992).
- [7] D. Atwood, L. Reina and A. Soni, Phys. Rev. D 55, 3156 (1997)
- [8] D. Atwood, L. Reina and A. Soni, Phys. Rev. D 53, 1199 (1996) [arXiv hep-ph/9506243]. W. S. Hou, G. L. Lin and C. Y. Ma, Phys. Rev. D 56, 7434 (1997).
- [9] S. Bejar, J. Guasch and J. Sola, Nucl. Phys. B 675, 270 (2003).
- [10] A. M. Curiel, M. J. Herrero, W. Hollik, F. Merz and S. Penaranda, Phys. Rev. D 69, 075009 (2004). A. M. Curiel, M. J. Herrero and D. Temes, Phys. Rev. D 67, 075008 (2003).
- [11] D. A. Demir, Phys. Lett. B 571, 193 (2003).
- [12] S. Bejar, F. Dime, J. Guasch and J. Sola, JHEP 0408, 018 (2004).
- [13] H. J. He, C. T. Hill and T. M. Tait, Phys. Rev. D 65, 055006 (2002).
- [14] For a review see e.g. J.F. Gunion, H.E. Haber, G.L. Kane and S. Dawson, The Higgs hunter's guide (Addison-Wesley), Redwood City, 1990.
- [15] A. G. Akeroyd, A. Arribas and E. Naimi, Eur. Phys. J. C 20, 51 (2001) [arXiv hep-ph/0002288]. A. Arribas and G. Moulhaka, Nucl. Phys. B 558, 3 (1999).
- [16] A. Denner, R. J. Guth, W. Hollik and J. H. Kuhn, Z. Phys. C 51, 695 (1991).
- [17] K. Hagiwara et al. [Particle Data Group], Phys. Rev. D 66 (2002) 010001.

- [18] P. Q. Hung, R. M. Coy and D. Singleton, *Phys. Rev. D* 50, 2082 (1994).
- [19] V. D. Barger, J. L. Hewett and R. J. Phillips, *Phys. Rev. D* 41, 3421 (1990); Y. Grossman, *Nucl. Phys. B* 426, 355 (1994).
- [20] P. Gambino and M. Misiak, *Nucl. Phys. B* 611, 338 (2001); F. M. Borzumati and C. Greub, *Phys. Rev. D* 58, 074004 (1998); *ibid* *Phys. Rev. D* 59, 057501 (1999);
- [21] A. G. Akeroyd, A. Arrib, E. M. Naimi, *Phys. Lett. B* 490, 119 (2000); A. Arrib, [hep-ph/0012353](http://hep-ph/0012353).
- [22] S. Kanemura, T. Kubota, E. Takasugi, *Phys. Lett. B* 313, 155 (1993);
- [23] G. Abbiendi et al. [OPAL Collaboration], *Eur. Phys. J. C* 18, 425 (2001).
- [24] G. Eilam, B. Haeri and A. Soni, *Phys. Rev. D* 41, 875 (1990).
- [25] T. Hahn, *Comput. Phys. Commun.* 140, 418 (2001); T. Hahn, C. Schappacher, *Comput. Phys. Commun.* 143, 54 (2002); T. Hahn, M. Perez-Victoria, *Comput. Phys. Commun.* 118, 153 (1999); J. Kublbeck, M. Bohm, A. Denner, *Comput. Phys. Commun.* 60, 165 (1990);
- [26] G. J. van Okenborgh, *Comput. Phys. Commun.* 66, 1 (1991); T. Hahn, *Acta Phys. Poln. B* 30, 3469 (1999)
- [27] A. Djouadi, J. Kalinowski and P. M. Zerwas, *Z. Phys. C* 70, 435 (1996).
- [28] A. G. Akeroyd, *Phys. Lett. B* 368, 89 (1996) [[arXiv:hep-ph/9511347](http://arxiv.org/abs/hep-ph/9511347)].
- [29] L. Brucher and R. Santos, *Eur. Phys. J. C* 12, 87 (2000).
- [30] I. F. Ginzburg, M. Krawczyk and P. Osland, *Nucl. Instrum. Meth. A* 472, 149 (2001). A. Djouadi, V. Driesen, W. Hollik and J. I. Illana, *Eur. Phys. J. C* 1, 149 (1998). A. Djouadi, V. Driesen, W. Hollik and A. Kraff, *Eur. Phys. J. C* 1, 163 (1998).
- [31] A. Arrib, W. Hollik, S. Penaranda and M. Capdequi Peyranere, *Phys. Lett. B* 579 (2004) 361.
- [32] S. Kanemura, Y. Okada, E. Senaha and C. P. Yuan, [arXiv:hep-ph/0408364](http://arxiv.org/abs/hep-ph/0408364). S. Kanemura, S. Kiyouura, Y. Okada, E. Senaha and C. P. Yuan, *Phys. Lett. B* 558, 157 (2003) [[arXiv:hep-ph/0211308](http://arxiv.org/abs/hep-ph/0211308)].